Inorganic Chemistry

ARTICLE

pubs.acs.org/IC

On the Oxidation of $EuFe_4Sb_{12}$ and $EuRu_4Sb_{12}$

Jessica M. Peddle, Michael W. Gaultois, and Andrew P. Grosvenor*

Department of Chemistry, University of Saskatchewan, Saskatoon, Saskatchewan, Canada S7N 5C9

ABSTRACT: Rare-earth-filled transition-metal pnictides having the skutterudite-type structure have been proposed for use as high-temperature thermoelectric materials to recover waste heat from vehicle exhaust, among other applications. A previous investigation by this research group of one of the most studied skutterudites, $CeFe_4Sb_{12}$, found that, when exposed to air, this material oxidized at temperatures that are considerably below the proposed maximum operating temperature. Here, by the combined use of TGA, powder XRD, and XANES, it has been found that the substitution of Ce^{3+} and Fe^{2+} for larger rare-earth and transition-metal elements (Eu^{2+} and Ru^{2+}) results in a significantly higher oxidation temperature compared to that of $CeFe_4Sb_{12}$. This increase can be related to the increased orbital overlap provided by these larger atoms (Eu^{2+} and Ru^{2+} vs Ce^{3+} and Fe^{2+}), enabling the development of stronger bonds. These results show how selective substitution of the constituent elements can significantly improve the thermal stability of materials.

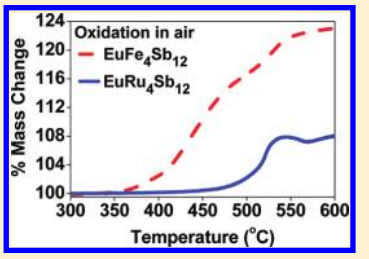

1. INTRODUCTION

To increase the fuel efficiency of vehicles without reducing the total power available for use, technologies are being (or have been) developed to convert waste energy to electricity.[1−3] Energy lost during braking can be recaptured and waste heat produced from vehicle exhaust can be converted to useful power.[4,5] Thermoelectric materials have been proposed for the conversion of waste exhaust heat to electricity.[2−4,6] For such applications, the maximum temperature that the device may be exposed to is relatively high (~500 °C) and, as such, it is important to develop materials that are stable under these harsh operating conditions.[1] Of the thermoelectric materials proposed for this application, p- and n-type rare-earth (RE) filled skutterudites (e.g., REM_4Pn_{12}; RE = La, Ce, Pr, Nd, Sm, Eu, Gd, Tb, Yb; M = Fe, Ru, Os; Pn = pnicogen = P, As, Sb) have received considerable attention because of their relatively high thermoelectric figure of merit at high temperatures.[3,6,8−11] (The figure of merit, ZT, describes the performance of a thermoelectric material.[6])

The cubic structure adopted by the RE-filled skutterudites (Figure 1) is based on that of the parent mineral phase, $CoAs_3$.[6,8,12] This structure contains tilted corner-sharing metal-centered octahedra and nearly square Pn_4 rings. The presence of Pn_4-rings in the structure leads to the formation of two distorted icosahedral cages per unit cell.[8] These cages can be occupied by RE atoms when the transition-metal sites are primarily occupied by group 8 elements (e.g., Fe, Ru, Os) with the charges usually represented as $RE^{3+}M^{2+}{}_4Pn^{1-}{}_{12}$ and the M atoms being low-spin (d^6).[6,8,13]

The ability of skutterudite-type materials to act as a thermoelectric can be related to their unique electronic structure and crystal structure. These materials are normally considered to be hole-doped (p-type), but substituting Co^{2+} or Ir^{2+} into the transition-metal site can lead to the development of n-type materials (e.g., $REFe_{4-x}Co_xSb_{12}$, $Ce_yRu_{4-x}Ir_xSb_{12}$), changing the primary charge carrier from holes to electrons.[6−8,14,15] The p-type RE-containing skutterudites are usually thought to contain one hole per formula unit (i.e., REM_4Pn_{12}) except when the RE is Eu. In this case, X-ray absorption near-edge spectroscopy (XANES) has shown Eu to be nearly divalent, which suggests the presence of ~2 holes per formula unit.[16−18] Rare-earth-filled skutterudites have low thermal conductivity but exhibit significant electrical conductivity.[6,8] These materials have historically been referred to as "phonon-glass, electron-crystals", with the reduced thermal conductivity being attributed to phonon scattering resulting from the RE atoms "rattling" in the icosahedral cage of Pn atoms.[6,8,19] Recent studies, however, have instead suggested that the RE-filled skutterudites might be better described as "phonon- and electron-crystals" with the reduced thermal conductivity resulting from a guest−host coupling interaction between the RE atoms *and* the M and Pn atoms.[20] Along with the properties listed above, these materials are also generally observed to be metals or narrow band gap semiconductors.[8]

A recent investigation of $CeFe_4Sb_{12}$ found that this material completely oxidizes when exposed to air at temperatures above 300 °C.[21] Although fabrication methods are such that thermoelectric devices are protected from the atmosphere, to increase the lifetime of these materials, it seems reasonable to attempt to enhance their resistance to high-temperature oxidation.[1,22] Such a resistance may be obtained through elemental substitution. It has been shown previously that $Ce_yRu_{4-x}Ir_xSb_{12}$ ($x < 1.5$) decomposes at much higher temperatures than $CeFe_4Sb_{12}$ under inert conditions; however, no investigation of the ability of these materials to resist oxidation has been completed.[7]

In this study, $EuFe_4Sb_{12}$ and $EuRu_4Sb_{12}$ have been examined to determine how the substitution of larger rare-earth and transition-metal atoms, compared to $CeFe_4Sb_{12}$, affects the temperature at which point these materials oxidize. Thermogravimetric analysis (TGA), powder X-ray diffraction (XRD), and XANES have been used to study the oxidation of these

Received: March 25, 2011
Published: June 08, 2011

 © 2011 American Chemical Society

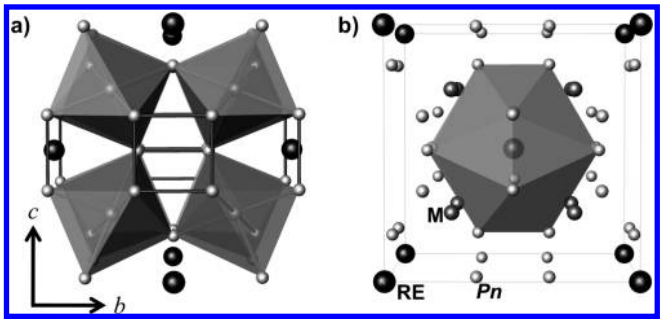

Figure 1. Representation of the structure adopted by the RE-filled skutterudites, REM_4Pn_{12} ($Im\bar{3}$) showing the formation of nearly square Pn_4 rings as well as the tilted MPn_6 octahedra (a) and the distorted icosahedral cage of Pn atoms, which can surround a RE atom (b). (The *a*-axis is directed out of the page.)

materials and to identify the oxidation products. The observations discussed herein provide important insight into how elemental substitution can influence the resistance of these materials to oxidation.

2. EXPERIMENTAL SECTION

2.1. Synthesis. $EuFe_4Sb_{12}$ and $EuRu_4Sb_{12}$ were synthesized via direct reaction of the elements (Eu, HEFA Rare-Earths Canada, 99.99%; Fe, Alfa Aesar, >99.9%; Ru, Smart-Elements, 99.97%; Sb, Alfa Aesar, 99.5%) in evacuated fused-silica ampules. An optimized heating profile was used to synthesize these materials.[23] The reactants were heated to 600 °C over 10 h and annealed at this temperature before the temperature was ramped to 1050 °C over 12 h to allow for proper mixing of the reactants, as this temperature is greater than the melting point of both Eu and Sb. After annealing these materials for >40 h at 1050 °C, they were quench-cooled in air. Once cool, the products were ground finely, sealed in new ampules, and annealed at 700 °C for >30 h. This final annealing temperature was used because the skutterudites generally decompose at temperatures above this value under inert environments.[23] $RuSb_2$ was synthesized to act as a standard by reacting stoichiometric amounts of Ru and Sb at 1050 °C in an evacuated fused-silica ampule. (For all synthesized materials, the initial reaction at 1050 °C was performed in acetone-pyrolyzed ampules to restrict the interaction between the elements and the silica ampules.) The purity of the synthesized materials was confirmed by powder X-ray diffraction (XRD) using a Rigaku Rotaflex RU-200 rotating anode powder XRD. Duplicates of each skutterudite material were synthesized, with some being observed to be phase pure while others were found to contain minor (<10%) contributions of $FeSb_2$ or $RuSb_2$ and/or Sb metal.

2.2. TGA and Powder XRD of Oxidized Materials. The air oxidation of $EuFe_4Sb_{12}$ and $EuRu_4Sb_{12}$ was investigated using a TA Instruments Q5000 TGA. Finely powdered samples of $EuFe_4Sb_{12}$ and $EuRu_4Sb_{12}$ were heated in air (flow rate = 25 mL/min) in a Pt pan from room temperature to 800 at 10 °C/min with the change in mass being constantly measured. The oxidation of $RuSb_2$ was also investigated using identical parameters to those listed above. Portions of each powdered Skutterudite were heated in air for two hours at temperatures ranging from 300 to 800 °C to further study the oxidation of these materials. (Oxidation temperatures were chosen based on examination of the TGA data.) Powder XRD was performed to identify the oxide phases formed using the instrument described above.

2.3. XANES. A previous investigation of the oxidation of $CeFe_4Sb_{12}$ found that many of the products formed are amorphous, requiring techniques other than powder XRD to identify them.[21] Eu and Ru L_3-edge XANES was used to investigate the materials oxidized in air at

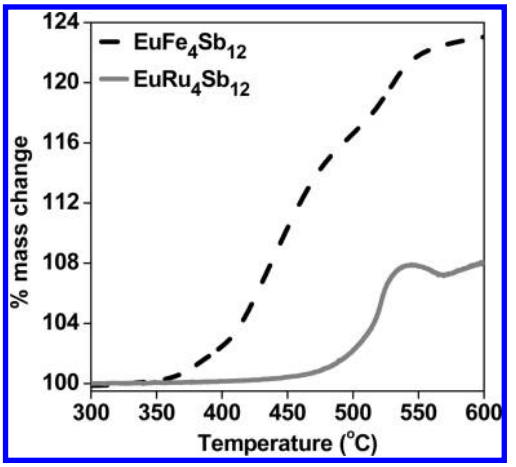

Figure 2. TGA profiles from $EuFe_4Sb_{12}$ and $EuRu_4Sb_{12}$ heated in air. A substantial increase in mass, resulting from oxidation, is observed at ~360 °C for $EuFe_4Sb_{12}$ and at ~460 °C for $EuRu_4Sb_{12}$.

specific temperatures, as the spectra are sensitive to the local coordination environment and do not require the presence of long-range order. XANES spectra were collected using the Pacific Northwest Consortium/X-ray Science Division-Collaborative Access Team (PNC/XSD-CAT, sector 20) bending magnet beamline (20BM) located at the Advanced Photon Source (APS), Argonne National Laboratory. Spectra from finely ground powders sandwiched between Kapton tape were collected using a Ge detector (fluorescence spectra) and N_2/He-filled ionization chambers (transmission spectra). Owing to the similarity in energy, the Eu L_3-edge spectra were calibrated by setting the peak maximum of the first derivative of the Fe K-edge spectrum from Fe metal foil to 7112.0 eV.[24] The Ru L_3-edge spectra were calibrated using Ru metal with an edge energy of 2838.0 eV.[24] The interpretation of spectra from the oxidized skutterudites was aided by comparison to spectra from standard materials containing the element of interest having different oxidation states and to phases either equivalent to or similar to those identified by powder XRD. The standard materials investigated were Eu_2O_3 (Alfa Aesar), Fe_2O_3 (Alfa Aesar), $RuSb_2$, RuO_2 (Alfa Aesar), $RuCl_3$ (Alfa Aesar), Sb_2O_3 (Alfa Aesar), and Sb_2O_5 (Alfa Aesar). All spectra were analyzed using the Athena software program.[25]

3. RESULTS AND DISCUSSION

3.1. TGA. If skutterudite materials are to be used in thermoelectric devices to convert waste heat to electricity under terrestrial conditions, it is important to understand how they react with the atmosphere at various temperatures. TGA was performed to study the resistance of these materials to oxidation at high temperatures, and plots representing the percent mass change versus temperature for $EuFe_4Sb_{12}$ and $EuRu_4Sb_{12}$ are presented in Figure 2. The mass of the materials studied was found to increase as the temperature was raised (i.e., oxidation occurs). When exposed to the atmosphere, significant oxidation of $EuFe_4Sb_{12}$ and $EuRu_4Sb_{12}$ begins above ~360 and ~460 °C, respectively. Both temperatures are considerably higher than the temperature at which $CeFe_4Sb_{12}$ begins to oxidize (~300 °C).[21]

The TGA profiles presented in Figure 2 show multiple changes in slope between ~360 and ~580 °C, which is likely because of the formation of different oxides at various temperatures (vide infra). The rate of change in mass for each sample slows above ~530 °C, which suggests that these skutterudites

dx.doi.org/10.1021/ic200619c |*Inorg. Chem.* 2011, 50, 6263–6268

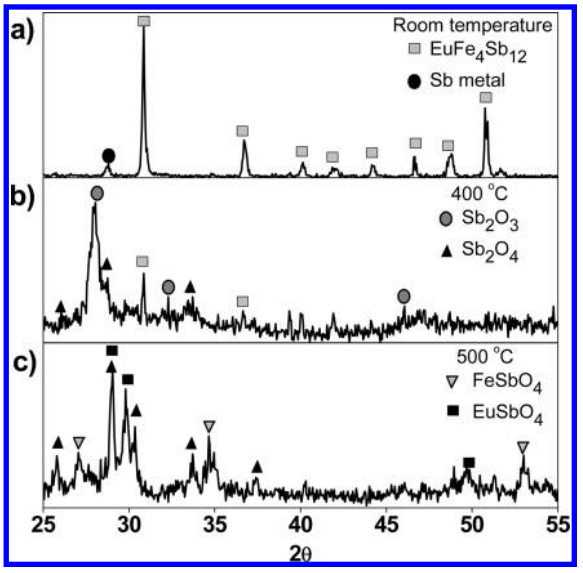

Figure 3. Powder XRD patterns from $Eu_4Fe_4Sb_{12}$ exposed to air at room temperature (a), 400 °C for 2 h (b), and 500 °C for 2 h (c). The different crystalline phases that were identified have been labeled using symbols. Oxides involving all of the constituent elements were not identified, suggesting the presence of some amorphous species.

have completely oxidized. (The slight dip observed at ~570 °C in the profile from $EuRu_4Sb_{12}$ may suggest sublimation of some of the oxidation products at high temperature, which is an unfortunate effect observed by many thermoelectric materials and can influence device reliability.[1,7]) The difference in mass change observed in $EuFe_4Sb_{12}$ versus $EuRu_4Sb_{12}$ is a result of the greater atomic mass of Ru.

3.2. Powder XRD. From the TGA results presented above, it can be easily seen that both $EuFe_4Sb_{12}$ and $EuRu_4Sb_{12}$ oxidize at temperatures much higher than $CeFe_4Sb_{12}$ does.[21] However, it is important to identify the oxidation products formed as this allows for an analysis of the relative bond strengths between the elements within the original material and an examination of whether all bonds within the structure are broken at similar temperatures. In this study, most of the oxidation products could be identified by analysis of the oxidized materials by powder XRD (see Figures 3 and 4).

3.2.1. $EuFe_4Sb_{12}$. Powder XRD patterns from $EuFe_4Sb_{12}$ after being exposed to air at room temperature (~25 °C) and at 400 and 500 °C for 2 h are presented in Figure 3. The powder XRD pattern presented in Figure 3a represents nearly pure-phase $EuFe_4Sb_{12}$. After exposure to air at 400 °C (Figure 3b), Sb_2O_4 and Sb_2O_3 were identified by powder XRD along with a small quantity of $EuFe_4Sb_{12}$. As no Eu- or Fe-bearing oxide phases were identified, it is likely that these materials are amorphous. (A similar observation was made for $CeFe_4Sb_{12}$ after being exposed to air at temperatures slightly above 300 °C.[21]) After exposure to air at 500 °C (Figure 3c), oxides containing all of the constituent elements were identified by powder XRD ($EuSbO_4$, $FeSbO_4$, and Sb_2O_4).

3.2.2. $EuRu_4Sb_{12}$. The powder XRD patterns from $EuRu_4Sb_{12}$ after exposure to air at room temperature and at 400, 500, and 600 °C for 2 h are presented in Figure 4. As mentioned in the Experimental Section, synthesized samples of $EuRu_4Sb_{12}$ were often found to contain low concentrations of $RuSb_2$ (see Figure 4a). After exposure of $EuRu_4Sb_{12}$ to air at 400 °C,

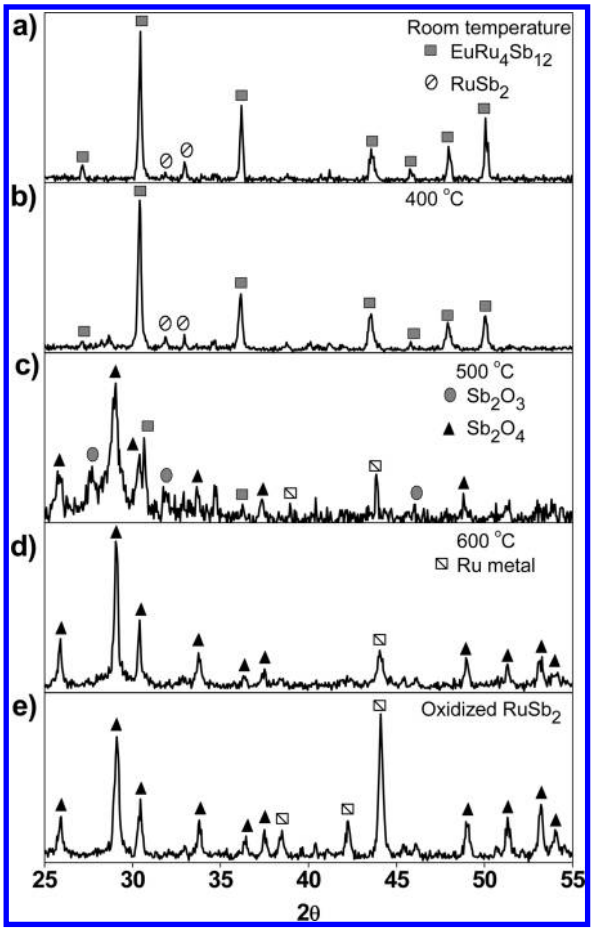

Figure 4. Powder XRD patterns from $Eu_4Ru_4Sb_{12}$ exposed to air at room temperature (a), 400 °C for 2 h (b), 500 °C for 2 h (c), and 600 °C for 2 h (d). The crystalline phases that were identified in the powder patterns have been labeled with symbols. To confirm the formation of Ru metal during the oxidation of $EuRu_4Sb_{12}$, the oxidation of $RuSb_2$ was investigated by TGA; the powder XRD pattern from $RuSb_2$ after the TGA experiment was complete is presented in part e.

only $EuRu_4Sb_{12}$ and $RuSb_2$ were identified in the corresponding powder XRD pattern (Figure 4b), confirming its increased resistance to oxidation compared to $EuFe_4Sb_{12}$ and $CeFe_4Sb_{12}$.[21] When $EuRu_4Sb_{12}$ was exposed to air at 500 °C, only Sb_2O_4, Sb_2O_3, *and* Ru metal were identified in the corresponding powder XRD pattern along with a minor quantity of $EuRu_4Sb_{12}$ (Figure 4c): no other ordered materials containing either Ru or Eu were observed. When $EuRu_4Sb_{12}$ was exposed to air at 600 °C, only Sb_2O_4 and Ru metal were unambiguously identified in the corresponding powder XRD pattern (Figure 4d). Weak intensity peaks that might suggest the presence of a very low concentration of $EuSbO_4$ (not labeled in Figure 4d) were also observed in this powder diffraction pattern.

The observation of Ru metal in the powder XRD patterns presented in Figure 4c,d was unexpected; however, such an identification was also made by examination of the powder XRD pattern collected from $RuSb_2$ after investigating its oxidation in air by TGA (Figure 4e). ($RuSb_2$ was observed by TGA to oxidize above 500 °C.) The formation of Ru metal has also been observed during the oxidation of RuAl-based alloys and is a result of the greater affinity of the other elements present to oxidize compared to Ru, which is a noble metal.[26]

dx.doi.org/10.1021/ic200619c |*Inorg. Chem.* 2011, 50, 6263–6268

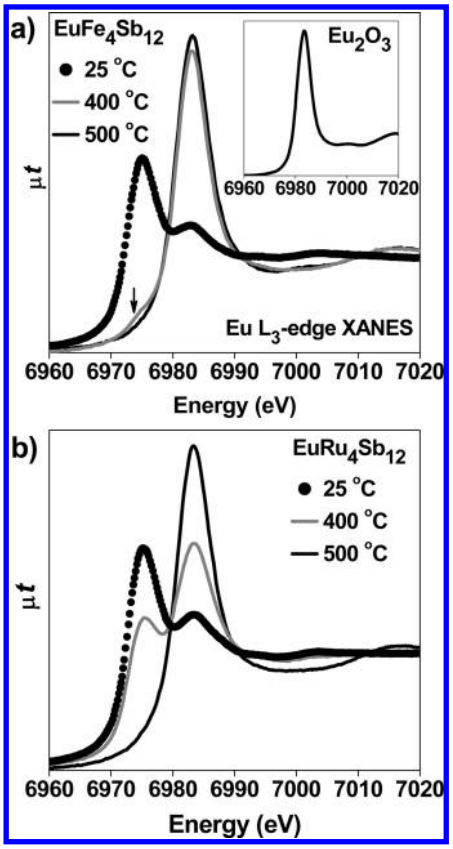

Figure 5. Eu L_3-edge XANES spectra from $EuFe_4Sb_{12}$ (a) and $EuRu_4Sb_{12}$ (b) before and after being exposed to air at high temperatures. To aid in the identification of the oxidation state of Eu in the oxidized and unoxidized materials, a standard spectrum from Eu_2O_3 was collected and is presented in the inset of part a.

3.3. XANES. Analysis of the oxidized skutterudites by powder X-ray diffraction allowed for a confirmation of the TGA results with most, but not all, of the oxidation products being determined. As some of the oxidation products were likely amorphous, techniques other than XRD were required to identify them, and Eu and Ru L_3-edge XANES spectra were collected.

3.3.1. Eu L_3-Edge. The Eu L_3-edge XANES spectra result principally from a $2p_{3/2} \rightarrow 5d$ excitation and have been investigated in the past to identify the oxidation state of Eu in EuM_4Sb_{12} (M = Fe, Ru, Os).[4] Through this analysis, some studies have concluded that Eu^{2+} and a minor concentration of Eu^{3+} are present while other studies suggested only the presence of Eu^{2+}.[14,16−18] Eu L_3-edge spectra from $EuFe_4Sb_{12}$ and $EuRu_4Sb_{12}$ before and after exposure to air at high-temperatures are presented in Figure 5. To aid in the determination of the Eu oxidation state of the oxidized materials, a standard spectrum from Eu_2O_3 was collected and is presented in the inset of Figure 5a.

3.3.1.1. Oxidation State of Eu in $Eu(Fe,Ru)_4Sb_{12}$. To understand how Eu in $EuFe_4Sb_{12}$ and $EuRu_4Sb_{12}$ oxidizes, it is important to first confirm its oxidation state in the unoxidized materials, which can be accomplished using Eu L_3-edge XANES. The Eu L_3-edge XANES spectra from both materials before exposure to air at high temperature (Figure 5a,b) show an intense peak centered at ∼6975 eV. This peak is significantly lower in energy than the main peak observed for Eu_2O_3 (see inset of Figure 5a) and confirms the predominantly divalent nature of Eu. (A decrease in oxidation state, and therefore an increase in screening of the nuclear charge, leads to a lower absorption energy.) Along with the high intensity peak located at ∼6975 eV, the spectra from unoxidized $EuFe_4Sb_{12}$ and $EuRu_4Sb_{12}$ also contain a low intensity, higher energy peak at ∼6983 eV (see Figure 5). Such a peak could correspond to the presence of a minor concentration of Eu^{3+}, as proposed previously (cf. the Eu_2O_3 spectrum presented in the inset of Figure 5a).[16−18] Alternatively, this higher energy peak has been described as being a satellite peak of the main Eu^{2+} excitation resulting from a final-state shakeup process.[14]

Shake-up satellite peaks, which are most often observed in X-ray photoelectron spectra (XPS), are a result of the transition of valence electrons to empty conduction states following the excitation of a core electron.[27] Examination of Eu 3d XPS spectra from EuF_3 and EuS suggests that the separation in energy between the main, core-line XPS peak and shakeup peak (∼2 eV) is smaller than the width of the most intense peak observed in the L_3-edge XANES spectrum of the unoxidized skutterudites (cf. Figure 5).[28] Also, as no higher energy satellite-peak was observed in the L_3-edge spectra from Eu_2O_3 (inset of Figure 5a), which would be expected if a shakeup peak were observable in these spectra, the presence of a shakeup peak in the Eu L_3-edge XANES spectra from the skutterudites is unlikely. The observations described above imply that, in agreement with previous studies, Eu^{2+} *and* Eu^{3+} are present in $EuFe_4Sb_{12}$ and $EuRu_4Sb_{12}$, with 2+ being the dominant oxidation state.[16−18]

3.3.1.2. Oxidation of Eu in $EuFe_4Sb_{12}$ and $EuRu_4Sb_{12}$. Along with confirming the oxidation state of Eu in the unoxidized materials, Eu L_3-edge XANES was also used to identify the oxidation state of the amorphous, Eu-containing oxidation products formed in these materials after being exposed to air at various temperatures. In agreement with both the TGA and powder XRD results, XANES spectra from $EuFe_4Sb_{12}$ and $EuRu_4Sb_{12}$ after exposure to air at temperatures ≥400 °C (Figure 5) have line shapes that are consistent with the oxidation of Eu^{2+} to Eu^{3+}.

Following exposure to air at 400 °C, the $EuFe_4Sb_{12}$ Eu L_3-edge spectrum is very similar to that of Eu_2O_3, but a low-energy shoulder is also observed (see arrow in Figure 5a). The observation of this shoulder implies the presence of a small contribution from Eu^{2+} and agrees with the corresponding powder XRD pattern (Figure 3b) in which a minor concentration of $EuFe_4Sb_{12}$ was observed. (No Eu oxides were detected by powder XRD (cf. Figure 3b), which indicates that the Eu^{3+} oxide was amorphous.) After exposure to air at 500 °C, the Eu L_3-edge spectrum from $EuFe_4Sb_{12}$ showed the presence of only Eu^{3+}, which was confirmed by the detection of $EuSbO_4$ by powder XRD (Figure 3c).

The Eu L_3-edge spectra from $EuRu_4Sb_{12}$ oxidized in air are presented in Figure 5b. The Eu L_3-edge spectrum from $EuRu_4Sb_{12}$ exposed to air at 400 °C for 2 h has two intense peaks corresponding to Eu^{2+} and Eu^{3+}. Such an observation implies that, although significant weight gain is not observed by TGA until temperatures above ∼460 °C are reached (see Figure 2), some oxidation of $EuRu_4Sb_{12}$ does occur. (Note that this discrepancy may also be a result of the material being held at 400 °C for 2 h, which is significantly longer than the time that it was held at this temperature during the TGA experiment.) After exposing $EuRu_4Sb_{12}$ to air at 500 °C, the Eu L_3-edge spectrum contained only a single peak, which corresponds to Eu^{3+} (Figure 5b).

dx.doi.org/10.1021/ic200619c |*Inorg. Chem.* 2011, 50, 6263–6268

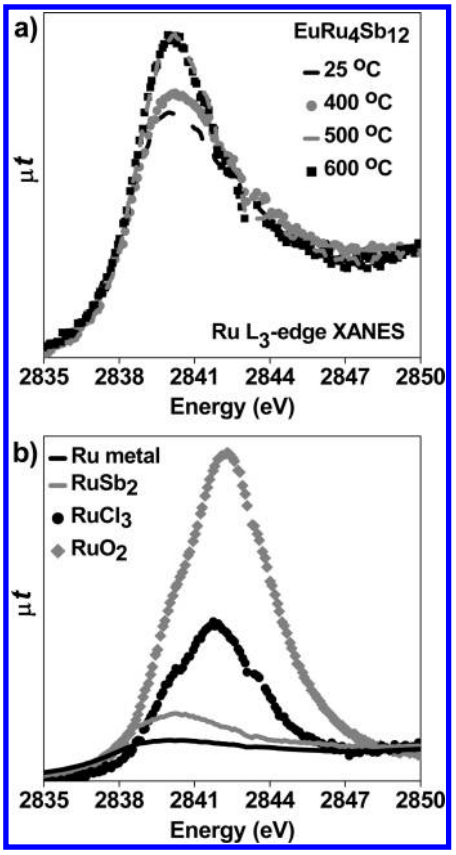

Figure 6. The Ru L_3-edge XANES spectra from $EuRu_4Sb_{12}$ before and after being exposed to air at high temperatures are presented in (a). To aid the examination of how the Ru oxidation state changes upon exposure to air at high temperature, spectra from standard materials having known oxidation states were collected and are presented in (b). The Ru L_3-edge spectra show an increase in energy and intensity with increasing oxidation state.

3.3.2. Ru L_3-Edge XANES from $EuRu_4Sb_{12}$. To identify the oxidation states of Ru in $EuRu_4Sb_{12}$ before and after exposure to air at various temperatures, Ru L_3-edge XANES spectra were collected and compared to materials having well-known oxidation states (Figure 6). As these spectra result from the excitation of 2p electrons to unoccupied 4d states, both the energy and intensity of the spectra yield information on the Ru oxidation state. The Ru L_3-edge spectrum from unoxidized $EuRu_4Sb_{12}$ is similar in energy and intensity to that of $RuSb_2$. After exposure to air at high-temperature, the Ru L_3-edge spectra became more intense and the peak maximum shifted to slightly higher energies (~0.2 eV). The increase in the peak intensity implies an increase in the average Ru oxidation state upon exposure to air at temperatures above 400 °C (cf. Figure 6a,b). As only Ru metal was detected by powder XRD in samples exposed to air at ≥500 °C (Figure 3), the higher oxidation state Ru-bearing materials detected by XANES are considered to be amorphous.

4. CONCLUSIONS

The oxidation of $EuFe_4Sb_{12}$ and $EuRu_4Sb_{12}$ has been investigated by TGA, powder XRD, and XANES and it was found that the temperature at which these materials begin to oxidize is significantly higher than for $CeFe_4Sb_{12}$.[21] With increasing ionic radius, the extent to which the valence orbitals from $Eu^{2+/3+}$ and Sb^{1-} *and* Ru^{2+} and Sb^{1-} overlap increases, compared to the equivalent Ce−Sb and Fe−Sb bonds in $CeFe_4Sb_{12}$.[29] This greater orbital overlap results in the development of stronger bonds that require more energy to break, relative to $CeFe_4Sb_{12}$, and as might be expected, the temperature at which point oxidation occurs increases. [Comparing the energies of bonds for equivalent interactions involving the elements present in the skutterudites investigated also allows for such a suggestion (e.g., the Ru−O and Fe−O bond energies are 528 ± 42 and 407 ± 1 kJ/mol, respectively).[30]] Along with investigating the oxidation of these materials, examination of the Eu L_3-edge XANES spectra from $EuFe_4Sb_{12}$ and $EuRu_4Sb_{12}$ before oxidation confirmed that, in agreement with previous studies, the oxidation state of Eu is primarily 2+, with a small concentration of 3+ also being present.[16−18]

The combined analysis of the materials investigated before and after oxidation by XANES and XRD has allowed for the observation that, at the initiation of oxidation, all bonds in the original materials are broken. This can be concluded on the basis of the fact that none of the oxidation products identified by XRD have isolated Fe/Ru−Sb or Eu−Sb bonds and that the amorphous materials detected by XANES have charges that are very different from the original materials. This implies that, compared to $CeFe_4Sb_{12}$, the substitution of $Eu^{2+/3+}$ for Ce^{3+} and/or Ru^{2+} for Fe^{2+} enables a strengthening of the bonds throughout the entire structure, allowing for an increased resistance to oxidation. The oxidation temperature was observed to increase more significantly when Ru replaced Fe then when Eu replaced Ce. This difference can be linked to the fact that the Eu−Sb bond lengths in these materials are long (~3.97 Å) compared to a nominal Eu−Sb bond (≥3.3 Å in $EuSb_2$ and Eu_2Sb_3).[16,31,32]

The usefulness of combining TGA analysis with XANES and powder XRD has been shown here, as the XANES spectra were able to detect that some oxidation of $EuRu_4Sb_{12}$ occurred before a significant weight increase was detected by TGA. Examination of $EuRu_4Sb_{12}$ by powder XRD was also able to track the formation of Ru metal during oxidation. Although the substitution of Ru increases the temperature at which the skutterudites oxidize, the possibility of Ru^{2+} being reduced to Ru^0 may exclude the usefulness of this element in thermoelectric materials, as the formation of Ru metal during operation could inhibit device performance.

Understanding the temperature range over which a material could oxidize is important to determining its applications and the level of protection needed from the environment to ensure device reliability. As has been shown here, substitution of the RE and M elements can greatly affect the temperature at which materials adopting the skutterudite-type structure oxidize. The challenge now will be to determine the proper level of substitution needed to increase the thermal stability of these materials without adversely affecting their thermoelectric properties. For example, $EuFe_4Sb_{12}$ oxidizes at a much higher temperature than $CeFe_4Sb_{12}$ does, but its ability to perform as a thermoelectric material is poorer.[8,33]

AUTHOR INFORMATION

Corresponding Author

*E-mail: andrew.grosvenor@usask.ca. Phone: (306) 966-4660. Fax: (306) 966-4730.

■ ACKNOWLEDGMENT

This work was supported by the Natural Sciences and Engineering Research Council (NSERC) of Canada through a discovery grant awarded to A.P.G. The University of Saskatchewan is also thanked for supporting this work through a new-faculty start-up grant awarded to A.P.G. Dr. Robert Scott (Department of Chemistry, University of Saskatchewan) is thanked for providing access to the TGA. Dr. Robert Gordon is thanked for help in carrying out XANES experiments at PNC/XSD-CAT, sector 20, at the APS. PNC/XSD facilities at the Advanced Photon Source and research at these facilities are supported by the US Department of Energy—Basic Energy Sciences, a Major Resources Support grant from NSERC, the University of Washington, Simon Fraser University, and the Advanced Photon Source. Use of the Advanced Photon Source is also supported by the U.S. Department of Energy, Office of Science, Office of Basic Energy Sciences, under Contract DE-AC02-06CH11357.

■ REFERENCES

(1) Yang, J.; Caillat, T. *MRS Bull.* **2006**, *31*, 224–229.
(2) Vining, C. B. *Nat. Mater.* **2009**, *8*, 83–85.
(3) Fleurial, J.-P. *JOM* **2009**, *61*, 79–85.
(4) Snyder, G. J.; Toberer, E. S. *Nat. Mater.* **2008**, *7*, 105–114.
(5) Demirdöven, N; Deutch, J. *Science* **2004**, *305*, 974–976.
(6) Nolas, G. S.; Merelli, D. T.; Tritt, T. M. *Annu. Rev. Mater. Sci.* **1999**, *29*, 89–116.
(7) Jewell, A. D.; Paik, J.-A.; Caillat, T. *Mater. Res. Soc. Symp. Proc.* **2006**, *886*, 369–374.
(8) Sales, B. C. In *Handbook on the Physics and Chemistry of Rare Earths*; Gschneidner, K. A., Jr., Bunzli, J.-C. G., Pecharsky, V. K., Eds.; Elsevier: Amsterdam, 2003; Vol. 33, pp 1−34.
(9) Ravi, V.; Firdosy, S.; Caillat, T.; Brandon, E.; van der Walde, K.; Maricic, L.; Sayir, A. *J. Electron. Mater.* **2009**, *38*, 1433–1442.
(10) Fleurial, J.-P.; Borshchevsky, A.; Caillat, T.; Ewell, R. *Proc. Intersoc. Energy Convers. Eng. Conf.* **1997**, *32*, 1080–1085.
(11) Caillat, T.; Fleurial, J.-P.; Borshchevsky, A. *Int. Conf. Thermoelectr.* **1996**, *15*, 100–106.
(12) Jeitschko, W.; Braun, D. *Acta Crystallogr. B* **1977**, *33*, 3401–3406.
(13) Grosvenor, A. P.; Cavell, R. G.; Mar, A. *Chem. Mater.* **2006**, *18*, 1650–1657.
(14) Grytsiv, A.; Rogl, P.; Berger, St.; Paul, Ch.; Bauer, E.; Godart, C.; Ni, B.; Abd-Elmeguid, M. M.; Saccone, A.; Ferro, R.; Kaczorowski, D. *Phys. Rev. B* **2002**, *66*, 094411/1–11.
(15) Sales, B. C.; Jin, R.; Mandrus, D.; Khalifah, P. *Phys. Rev. B* **2006**, *73*, 224435/1–8.
(16) Bauer, E. D.; Ślebarski, A.; Frederick, N. A.; Yuhasz, W. M.; Maple, M. B.; Cao, D.; Bridges, F.; Giester, G.; Rogl, P. *J. Phys.: Condens. Matter.* **2004**, *16*, 5095–5107.
(17) Krishnamurthy, V. V.; Keavney, D. J.; Haskel, D.; Lang, J. C.; Srajer, G.; Sales, B. C.; Mandrus, D. G.; Robertson, J. L. *Phys. Rev. B* **2009**, *79*, 014426/1–8.
(18) Krishnamurthy, V. V.; Lang, J. C.; Haskel, D.; Keavney, D. J.; Srajer, G.; Roberston, J. L.; Sales, B. C.; Mandrus, D. G.; Singh, D. J.; Bilc, D. I. *Phys. Rev. Lett.* **2007**, *98*, 126403/1–4.
(19) Chakoumakos, B. C.; Sales, B. C.; Mandrus, D.; Keppens, V. *Acta. Crystallogr. B* **1999**, *55*, 341–347.
(20) Koza, M. M.; Johnson, M. R.; Viennois, R.; Mutka, H.; Girard, L.; Ravot, D. *Nat. Mater.* **2008**, *7*, 805–810.
(21) Sklad, A. C.; Gaultois, M. W.; Grosvenor, A. P. *J. Alloys Compd.* **2010**, *505*, L6–L9.
(22) Stark, I.; Stordeur, M. *Int. Conf. Thermoelectr.* **1999**, *18*, 465–472.
(23) Sales, B. C.; Mandrus, D.; Chakoumakos, B. C.; Keppens, V.; Thompson, J. R. *Phys. Rev. B* **1997**, *56*, 15081–15089.
(24) Thompson, A.; Attwood, D.; Gullikson, E.; Howells, M.; Kim, K.-J.; Kirz, J.; Kortright, J.; Lindau, I.; Peanetta, P.; Robinson, A.; Scofield, J.; Underwood, J.; Vaughan, D.; Williams, G.; Winick, H. *X-ray Data Booklet*; Lawrence Berkeley National Laboratory, University of California: Berkeley, CA, 2001.
(25) Ravel, B.; Newville, M. *J. Synchrotron Radiat.* **2005**, *12*, 537–541.
(26) Cao, F.; Nandy, T. K.; Stobbe, D.; Pollock, T. M. *Intermetallics* **2007**, *15*, 34–43.
(27) Michels, G.; Junk., S.; Schlabitz, W.; Holland-Moritz, E.; Abd-Elmeguid, M. M.; Dünner, J.; Mewis, A. *J. Phys.: Condens. Matter* **1994**, *6*, 1769–1778.
(28) Vercaemst, R.; Poelman, D.; Fiermans, L.; Van Meirhaeghe, R. L.; Laflère, W. H.; Cardon, F. *J. Electron Spectrosc. Relat. Phenom.* **1995**, *74*, 45–56.
(29) Shannon, R. D. *Acta Cryst. A* **1976**, *32*, 751–767.
(30) Luo, Y.-R. In *CRC Handbook of Chemistry and Physics*, 91st ed.; Haynes, W. M., Ed.; CRC Press: Boca Raton, FL, 2011; pp 9-65−9-98.
(31) Hulliger, F.; Schmelczer, R. *J. Solid State Chem.* **1978**, *26*, 389–396.
(32) Chapuis, G.; Hulliger, F.; Schmelczer, R. *J. Solid State Chem.* **1980**, *31*, 59–67.
(33) Kuznetsov, V. L.; Rowe, D. M. *J. Phys.: Condens. Matter* **2000**, *12*, 7915–7921.